IJARSCT
ISSN (Online) 2581-9429
International Journal of Advanced Research in Science, Communication and Technology (IJARSCT)
International Open-Access, Double-Blind, Peer-Reviewed, Refereed, Multidisciplinary Online Journal
Impact Factor: 7.301
Volume 8, Issue 1, August 2023

Reliability Study of Reinforced Concrete Structures Under Carbonation Attack

Samarjeet Saket[1] and Prof. Lavina Talvade[2]
Student, Master of Technology in Structure Engineering
Shiv Kumar Singh Institute of Technology & Science, Indore

Abstract: *The enhanced performance due to the addition of steel within concrete elements has thrust reinforced concrete structures to be one of the most commonly used construction materials in the world. Reinforced concrete structures are exposed to a variety of deterioration mechanisms during their operational existence, each of which contributes to reducing their service life, durability, and load bearing capacity. The longevity of these reinforced concrete structures is strongly connected to degradation processes, whose origin is environmental and/or functional. Among these processes is the initiation and evolution of corrosion on the steel reinforcement. Steel reinforcement has direct effects on the durability, safety, and useful service life of a reinforced concrete structure. The reliability of an engineering design is measured by the probability that a design meets certain demands under certain conditions, or its resistance will be able to sustain given loads. The main focus of this study is to develop a reliability-based service life prediction model using the uncertainties characteristically recognized in the parameters included in established corrosion detection processes. Reliability algorithms, such as Advanced First Order Reliability Method (AFORM), were used to analyze the effects of key factors within both uniform and localized corrosion conditions on time- dependent reliability. The results clearly illustrate the decrease in reinforced concrete element reliability after exposure to corrosion due to the reduction in flexural capacity of the steel reinforcement*

Keywords:. Christian Mission, Anglican Church, Civilizing Mission, Romanticism, Eastern and Orient

I. INTRODUCTION

Concrete advantages, such as versatility and competitive cost, have given concrete a practical advantage when compared to other structural materials. With the enhanced addition of steel for structural ductility and tensile resistance, reinforced concrete has been the most widely used construction materials in the world since the 1950's (Liberati 2014). Construction methods, mathematical/analysis models and design codes for the design of reinforced concrete structures seem to be well developed in the modern era of engineering. Safety, economic and functionality requirements are heavily considered throughout the design process. Another important factor to plan for when designing a structure is the structural durability. The durability of reinforced concrete structures is strongly connected to degradation processes whose origin is environmental and/or functional. Among these processes is the development of corrosion on the steel reinforcement. Corrosion is a complex, mechanical degradation process that occurs in metallic materials as a result of chemical or electrochemical actions (Farsani 2015).

Reinforcement corrosion has a direct effect on the durability of reinforced concrete structures. Corrosion of reinforcing bars is one of the major causes of deterioration of reinforced concrete structures; affecting the useful service life of a given structure. Two types of corrosion, general and pitting, are possible (Kioumarsi 2017). General corrosion affects the cross section of reinforcement with nearly uniform metal loss over the perimeter of reinforcing bars. It also causes cracking and eventual spalling of the concrete cover and produces rust staining on the concrete surface, making it easily detectable during inspection of the structure. Pitting, also referred to as localized corrosion, concentrates over small areas of reinforcement. Pitting corrosion often does not cause disruption to the concrete cover and produces little rust staining on the concrete surface, making it slightly more difficult to be discovered during inspections (Ghanooni-Bagha 2017).

IJARSCT
ISSN (Online) 2581-9429
International Journal of Advanced Research in Science, Communication and Technology (IJARSCT)
International Open-Access, Double-Blind, Peer-Reviewed, Refereed, Multidisciplinary Online Journal
Impact Factor: 7.301
Volume 8, Issue 1, August 2023

Structural reliability and risk analysis aim at quantifying the probability of failure taking into account relevant uncertainties. These uncertainties in a system vary from design to manufacturing to environmental conditions. The modeling of structural systems considering these uncertainties has become useful regarding the durability of a structure. Probability models can embrace knowledge from multiple fields to allow for a more consistent, comprehensive and dependable understanding concerning the reliability of a structure as opposed to using a purely deterministic approach. This method acknowledges the addition of uncertainties in numerous analyses in a consistent theoretical manner through statistical associations (Liberati 2014).

This research aims to develop a framework of analysis focusing on corrosion- affected reinforced concrete members and systems, specifically evaluating the reliability levels stemming from deterioration of steel reinforcement undergoing general and localized corrosion degradation processes within reinforced concrete girders of multiple highway bridges. The developed framework can be applied to any design limit states that can be affect by corrosion. However, only flexural strength limit states are considered in this study.

Computational tools, such as MATLAB, were employed using the First Order Reliability Method to gauge the serviceability of the selected design space of reinforced concrete girders enduring uniform and pitting corrosion conditions. The different corrosion conditions and varying design spaces, further discussed in Chapter 3 of this paper, used probabilistic corrosion models from literature review as a basis of material to be input into MATLAB to evaluate the integrity or serviceability of a reinforced concrete girder. No concrete deterioration or loss of bond strength at the concrete to steel interface was taken into account. The developed framework can be used by infrastructure owners to assist in their decision making process to project the existing life of reinforced concrete materials experiencing corrosion degradation. Based on these projections, owners can also plan intervention strategies to mitigate corrosion or strengthen the affected members.

As of 1998, there were 583,000 bridges in the United States. Of these, 200,000 were steel; 235,000 were standard reinforced concrete; and 108,000 were prestressed concrete. At this time, it was estimated that nearly 15 percent of bridges were structurally deficient, predominantly due to the corrosion of steel and steel reinforcement. The annual direct cost of corrosion for highway bridges in 1998 was estimated at $8.3 billion (Koch et al., 2002). Indirect costs to users of this infrastructure can be account with time and lost productivity spent in traffic delays.

With an understanding of the corrosion process as well basic chemical and reinforced concrete concepts, reliability algorithms can be established and analyzed using established methodologies such as the First Order Reliability Method (FORM). These methods have the ability to determine the probability of structural failure. The approximation of structural failure probability can be used for estimating the performance and lifetime of structures. The primary goal of this research is to analyze the corrosion of steel reinforcement within a reinforced concrete structure, specifically within an individual girder of a bridge under flexure loading conditions, and the concerns it will yield regarding the structures' reliability.

II. LITERATURE REVIEW

Corrosion of the reinforcement embedded in concrete causes most of the failures of reinforced concrete structures. Up until about half a century ago, carbonation of the concrete was considered to be the main cause of corrosion. Since then, chloride-induced corrosion has become much more renowned, especially for structures exposed to chloride-containing environments, i.e. deicing salt, marine climate, or salt-contaminated aggregates (Böhni 2005). As previously mentioned, corrosion of the reinforcement can present itself through different forms, ranging from widespread, general corrosion to a more localized attack, referred to as pitting corrosion. General corrosion is associated mostly in cases of carbonated concrete, whereas pitting corrosion is commonly instigated by chloride ions resulting in pits randomly distributed along steel bars. The depth of these pits in steel bars may become large before any signs of deterioration appear on concrete surfaces, making it an extremely serious issue. Deterioration caused by reinforcement corrosion is normally divided into two main timeframes: initiation and propagation.

Along the surface of an embedded steel bar, when there exists a difference in electric potential, the surrounding concrete acts as an electrochemical cell consisting of anodic and cathodic regions of the steel with the pore water in the hardened cement paste acting as an electrolyte. Goyal et al. (2018) describes that this process generates a flow of current through the system, causing an attack on the metal with more negative electrode potential, i.e. the anode, while

IJARSCT
ISSN (Online) 2581-9429
International Journal of Advanced Research in Science, Communication and Technology (IJARSCT)
International Open-Access, Double-Blind, Peer-Reviewed, Refereed, Multidisciplinary Online Journal
Impact Factor: 7.301
Volume 8, Issue 1, August 2023

the cathode remains undamaged. Thus, the corrosion of the reinforcement is initiated as depicted in Figure 1 Böhni (2005) notes the occurrence of the corresponding chemical reactions in the following equations.

Anodic Reaction: $2Fe \rightarrow 2Fe2+ + 4e-$ (1)

Cathodic Reaction: $O2 + 2H2O + 4e- \rightarrow 4OH-$ (2)

Reaction Sum: $2Fe + 2H2O + O2 \rightarrow 2FE(OH)2$ (3)

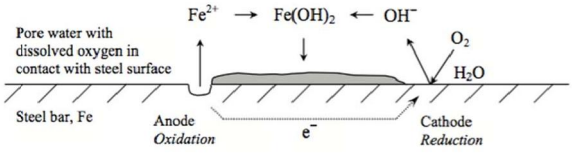

The anodic reaction from Equation 1 represents the dissolution of the metal. The flux of ions and electrons respectively can be taken as a measure of the corrosion rate. The corrosion rate is customarily given as mass lost per unit of time and area, reduction of the thickness per unit of time or as current density (current per unit of area). Figure 1 and Equations 1-3 provide a chemical approach of defining corrosion initiation. A more basic explanation for the period of corrosion initiation can be labeled as the time from the end of construction until the activation of the corrosion process, i.e. when the protective layer, which ensures the adhesion between concrete and steel, is destroyed in the presence of moisture and oxygen. This period can be modeled using a pure diffusion process using Fick's second law under the assumption that concrete is a homogenous and isotropic material (Bamforth 2000; Tutti 1982).

Following the corrosion initiation period is the propagation phase. This stage is recognized as the time required for corrosion to cultivate to the extent at which the load capacity of the structural member becomes insufficient (Shayanfar et al. 2015). During this phase, the corrosion of the steel reinforcements leads to the reduction of reinforcement cross-sections prompting a drop in strength of the reinforced concrete member (Markeset and Mydral 2008). The formation of rust on the reinforcement then leads to concrete cracking in the proximity of other steel bars. The development of cracks stimulates a loss of bond strength at the steel to concrete interface and remains until spalling of the concrete cover transpires (El Hassan et al. 2010).

2.1 Carbonation Induced Corrosion

Porosity, a measure of the void spaces in a given material, of concrete ranges on a minuscule scale, typically from the micrometer to nanometer level (Nóvoa 2016). Within the pores of concrete, there is obviously some liquid water, but there is also adsorbed and structural water. Goyal et al. (2018) explains that the presence of the adsorbed and structural water can affect the structural and mechanical properties of the concrete. The natural reactivity and porous structure of concrete make it prone to natural degradation.

Of these degradation processes exists carbonation, which refers to the penetration of carbon dioxide into the concrete layer and the subsequent neutralization of alkalis, such as calcium carbonate, in the pore fluid (Zhou et al. 2015)

Consequently, carbonation causes a reduction in the pH level of concrete. A necessary pH of concrete for sufficient corrosion protection is usually around 11-11.5; however, after the carbonation process, the pH could fall to around 9.0 (Böhni 2005). At a pH level of this magnitude, the passive layer will not be stable and thus, corrosion is likely to occur if sufficient oxygen and water are present in the vicinity of the reinforcement (Heiyantuduwa et al. 2006).

Corrosion induced by carbonation is expected to be much more uniform than corrosion that is chloride-induced (Cairns et al. 2005).

2.2 Chloride induced corrosion

The steel reinforcement will remain in a passive sate so long that it is embedded in a sound concrete layer; however, the passive state no longer exists when the concrete around it begins to deteriorate. With a lack of surrounding concrete, chloride ions may penetrate from the environment and be able reach the reinforcement. As chloride ions penetrate into concrete, the alkalinity near the steel reinforcement will increase as represented in aforementioned Equation 2. Goyal et al. (2018) expresses that to maintain electro-neutrality, chloride and hydroxide ions diffuse to the interface. With these diffusion movements, the chloride ion concentration will build up close to the surface, yielding saturation at the

IJARSCT
ISSN (Online) 2581-9429
International Journal of Advanced Research in Science, Communication and Technology (IJARSCT)
International Open-Access, Double-Blind, Peer-Reviewed, Refereed, Multidisciplinary Online Journal
Impact Factor: 7.301
Volume 8, Issue 1, August 2023

interface of Fe2+, iron, and Cl–, chloride. This will shift the electric potential in a more cathodic direction (Popov 2015). This process is known as chloride-induced corrosion.

The chloride content required for steel depassivation and corrosion initiation is referred to as the critical chloride content or the chloride threshold value (Goyal et al.

2018). Once the chloride ion concentration goes beyond the threshold value, the passive layer will locally be destroyed, which results in localized corrosion (Bertolini et al. 2018). The critical threshold depends on various factors including but not limited to: concrete quality, temperature, moisture content, and concrete cover (El Hassan et al. 2010).

According to Angst et al. (2009), there are actually multiple ways to define the critical chloride threshold. Scientifically speaking, the critical chloride content can be defined as the chloride content required for the depassivation of steel. From an engineering standpoint, the chloride threshold value is the chloride content associated with visible or tolerable deterioration of the reinforced concrete structure. Yet, both of these critical chloride definitions relates to different circumstances. The scientific designation of a chloride threshold only includes a depassivation criterion, which means only the corrosion initiation stage is considered, while the engineering description of the threshold considers part of the propagation stage in addition to the initiation stage. Therefore, the two definitions of chloride threshold lead to different critical chloride content values as shown in Figure 2. Figure 2 clearly shows that different definitions of the critical chloride lead to separate critical chloride values, where the engineering outlook leads to a higher chloride threshold value. The scientific view of the threshold is more detailed and approximate since it relates only to the chloride content related to depassivation.

However, the chloride content related to the engineering view remains unclear since the amount of tolerable deterioration is ambiguous.

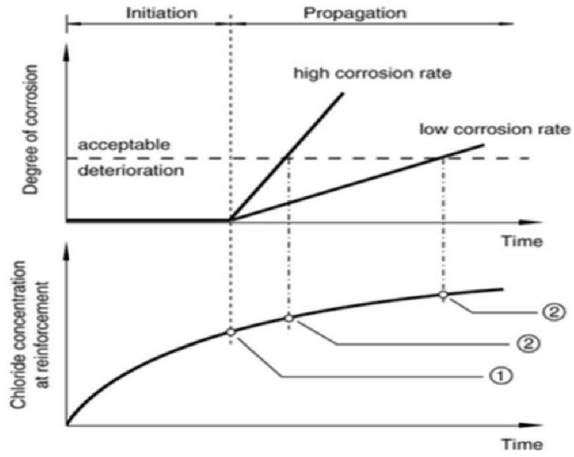

For these reason, the critical chloride threshold value is an unclear component of this corrosion process. Since the pH of concrete varies according to the concrete composition of the concrete, e.g. type of cement or water to cement ratio, results reported in the literature scatter over a large range, and therefore, no fixed or single value for this threshold is comprehensively accepted (Böhni 2005). Though, a popular approach to quantify the critical chloride threshold level is based on Fick's second law, which requires knowledge of the diffusion coefficient of the cement-based material (Poupard et al. 2004).

The effects of chloride diffusion are more thoroughly examined due to its' threatening nature. Therefore, accurately modeling the chloride diffusion will be essential to better evaluate the corrosion on steel reinforcement. Due to the inherent randomness regarding chloride diffusion and corrosion, these processes should be properly modeled using probabilistic approaches (Liberati et al. 2014). Ghanooni-Bagha et al. (2017) introduce a probabilistic model for predicting corrosion initiation and propagation. The time to corrosion initiation, using Fick's second diffusion law due to its' accuracy, can be calculated using Equations 4 and 5 by simulating the chloride ingress in concrete (Almusallam 2001; Bastidas-Arteaga et al. 2009).

IJARSCT
ISSN (Online) 2581-9429
International Journal of Advanced Research in Science, Communication and Technology (IJARSCT)
International Open-Access, Double-Blind, Peer-Reviewed, Refereed, Multidisciplinary Online Journal
Impact Factor: 7.301
Volume 8, Issue 1, August 2023

2.3 Detection and protection techniques against corrosion

It is important to be proactive in identifying and rehabilitating corrosion-affected reinforced concrete members. Repairs to corrosion-damaged concrete structures are typically categorized into two methods: conventional repair and electrochemical (Goyal et al. 2018). Conventional methods for concrete repair aim at removing all chloride-contaminated or carbonated concrete, cleansing the steel and reorganizing the surface with fresh, chloride-free and alkaline, cementitious concrete or mortar. Geiker and Polder (2016) concluded that though these are generally temporary techniques for corrosion prevention, there is downside to these methods as they can lead to acceleration of corrosion in nearby repaired areas. Unless all chloride is removed, especially from steel surfaces where corrosion pits may lie, corrosion will likely reinitiate after a short duration (Böhni 2005). For these reasons, Elsener and Angst (2007) declares that these methods are commonly costly and not as effective as electrochemical methods. In electrochemical techniques, the chemical reactions and current flows due to corrosion are restrained by the application of an external direct current supply with the assistance of an anode. The direct current passes from the artificial anode as a flow of ions through the pore water of the concrete to the reinforcing steel (Drewett et al., 2011). Some effective electrochemical techniques for corrosion prevention and mitigation include: cathodic protection, cathodic prevention, electrochemical realkalization and electrochemical chloride removal.

Furthermore, some steps or practices can be taken earlier than expected, including during the construction of reinforced concrete structures. To prevent corrosion of reinforcement in concrete, an alternative reinforcement that is made of corrosion-resistant material could be utilized, e.g. stainless steel or fiber-reinforced plastic amongst other types (Goyal et al. 2018). The corrosion resistance of stainless steel bars is significantly higher than carbon or mild steel because of the higher stability of their passive film, which is high in chromium and is self-healing in an oxygen rich environment (The Concrete Society, 1998). Alternatively, fiber-reinforced plastic (FRP reinforcement) are composite materials; which have high corrosion resistance, are light weight, and generally have a high tensile strength (ACI, 2007) and can be used as internal reinforcement for concrete structures. Additionally, adding coatings to steel or concrete can serve as a physical barrier to corrosion. Cicek (2018) states that coatings, sometimes referred to as sealers, have higher adhesion and are non-reactive in a corrosive environment and protect steel from any mechanical damages.

2.4 Structural Reliability and Probabilistic Evaluation

Structures are complex systems that are susceptible to a number of uncertainties at all phases of design execution as well as practical usage. Some uncertainties can never be completely eliminated and must, therefore, be taken into account when designing or validating the integrity of a structure. Some common sources of uncertainties include: lack of reliable experimental data (i.e., statistical uncertainty), environmental influences, geometrical data, randomness of actions, and gross errors in design. Numerous design methods and operative techniques have been proposed and utilized worldwide in an effort to predict and control the unfavorable effects of underlying uncertainties within the duration of a structure's service life. As a by-product, the theory of structural reliability has been developed to evaluate uncertainties within a structural system in a rational way and to consider when designing and monitoring structural performance.

Reliability is the ability of a structure to satisfactorily meet given requirements under specified conditions during the intended design life (Holický, 2009). Essentially, a structure should maintain its' integrity for the usage of which it was required as well as sustaining all actions and influences likely to occur during construction and usage during its' intended working life.

III. METHODOLOGY

Now knowing fundamental information regarding corrosion and structural reliability, this chapter displays the design spaces and methods that are set up in order to evaluate the ramifications that the corrosion process has on steel reinforcement.

3.1 Design Space

With the goal of evaluating cases of both uniform and localized corrosion surrounding varying design specifications, approaches and methods of past and current researchers are herein utilized. A design space used by Okeil et al. (2013) was selected to ensure that the design equations and methods convey acceptable reliability levels over a wide range of

IJARSCT
ISSN (Online) 2581-9429
International Journal of Advanced Research in Science, Communication and Technology (IJARSCT)
International Open-Access, Double-Blind, Peer-Reviewed, Refereed, Multidisciplinary Online Journal
Impact Factor: 7.301
Volume 8, Issue 1, August 2023

distinctive design scenarios. Three different bridges were chosen for these scenarios. Each bridge varies in span length, but each contains five, typical reinforced concrete girders spaced transversally seven feet laterally from each other, as can be seen in Figure

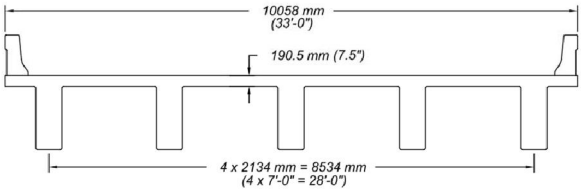

In Figure. Details of typical bridge used to cover design space (Okeil et al, 2013) The span length for each considered bridge is 45 feet, 60 feet, and 75 feet, or 13.72 meters, 18.29 meters, and 22.86 meters, respectively. A singular interior reinforced concrete girder from each particular bridge, as shown in Figures 7-9, will be analyzed using the following approaches. The nominal flexural demands on the selected beams are found in Tables 7-9. More details on these design spaces can be found elsewhere in Okeil et al. 2013.

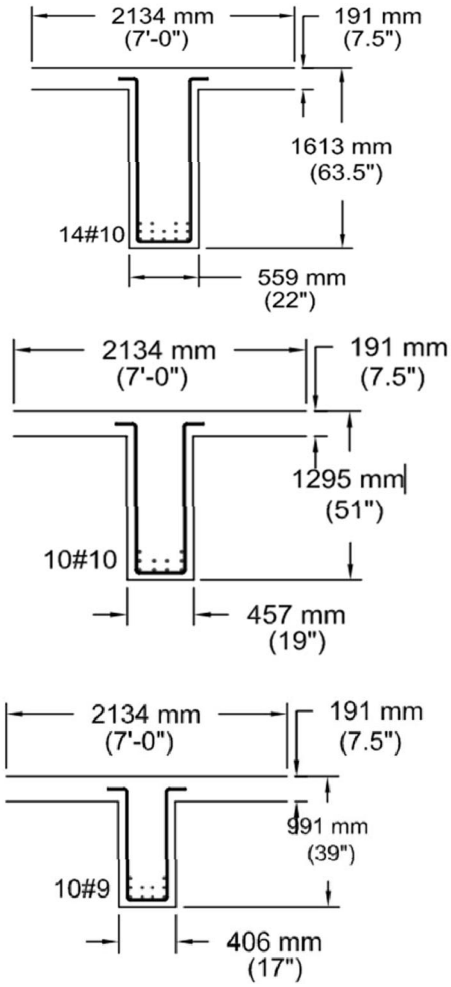

3.2 Design Approach

The diffusion coefficient is dependent on conditions such as concrete material properties, water to cement ratio, and exposure conditions. However, Castaneda et al. (2018) shifted focus on developing an effective, probabilistic model using the least number of parameters based on model selection criteria for developing the diffusion coefficient in a

IJARSCT
ISSN (Online) 2581-9429
International Journal of Advanced Research in Science, Communication and Technology (IJARSCT)
International Open-Access, Double-Blind, Peer-Reviewed, Refereed, Multidisciplinary Online Journal
Impact Factor: 7.301
Volume 8, Issue 1, August 2023

manner where it would not be a deterministic, constantly held value such as portrayed by Equation 6. Bayesian methodology was utilized within the evidence- based models using experimental data. The impacts of each parameter including material properties, environmental conditions, and the structural geometries were invetigated considering the uncertianties within the system. A statistical approach was added utilizing Bayesian updating technique to decide the model parameters. The model parameters, $\theta 1$, $\theta 2$, and $\theta 3$, were estimated by the maximization function that maximizes the concentration profile likelihood when previous reference case data set was given. Still using Fick's law (Liberati, 2014, Nogueira, 2012), Equations 44 and 45 were established by Castaneda et al. (2018).

controlled most cost- effectively. When the study is complete, management must then decide whether to implement any recommended risk reduction measures to achieve its risk goals.

$C(x, t) = C\ (1 — erf$ x $2\sqrt{}$Dt) (44)

$D(t) = \theta 1(\theta 3/t)\theta 2$ (45)

where, $C(x, t)$ = Chloride concentration (% mass),

Cs = Chloride concentration on concrete surface (% mass),

x = Distance from surface (mm),

D = Chloride diffusivity (mm2/month),

t = Time (month), and

$\theta 1$, $\theta 2$, $\theta 3$ = Parameters in the diffusion model

Table 1 displays the consequent statistics of the parameters for the chloride diffusion model using the reference case of WC = 0.46 and 7 days of curing, based on the diffusion equation without the correction factor. Sigma, σ, represents the model error. The correlation coefficient shows the parameters' correlation with one another. In this case, $\theta 2$ and $\theta 3$ shows relatively higher correlation compared to other parameters' correlation, which means that those two parameters are possibly merged to increase the equation efficiency, but there is also other possibility that such a merging process increases the model uncertainty. It was observed that the model has low statistical uncertainty as is evident by the generally low standard deviation values.

			Correlation Coefficient		
	Mean	Std. Dev.	θ_1	θ_2	θ_3
θ_1	500	1	1	0.013	-0.213
θ_2	30	1.13	0.013	1	-0.26
θ_3	0.56	0.027	-0.213	-0.26	1
σ	0.342	0.019	0.019	-0.336	0.044

In order to express the different concrete conditions compared to the reference case, the correction factors, α1 and α2, from Tables 2 and 3 were added on the diffusivity equation. The correction factor helped improve the model fit to the given data set, and reflects the trend that may not be observed in the posterior statistics with reference case. The factors, α1 and α2, represent a water to cement ratio correction factor and curing day correction factor, respectively.

Table 2. Water to cement ratio correction factor

WC Correction Factor, α_1			
WC Model	Distribution	α_1Mean	α_1Std. Dev.
0.46	Normal	1	0.4
0.5	Normal	1.719	0.576
0.53	Normal	2.283	0.673
0.7	Normal	2.678	-
0.76	Normal	2.783	0.984

Table 3. Curing day correction factor

Curing Days Correction Factor, α_2			
C_d Model	Distribution	α_2Mean	α_2Std. Dev.
1	Normal	1.265	0.221
3	Normal	0.716	0.073
7	Normal	0.875	0.09

ISSN 2581-9429 IJARSCT

IJARSCT
ISSN (Online) 2581-9429
International Journal of Advanced Research in Science, Communication and Technology (IJARSCT)
International Open-Access, Double-Blind, Peer-Reviewed, Refereed, Multidisciplinary Online Journal
Impact Factor: 7.301
Volume 8, Issue 1, August 2023

Using these correction factors and model parameters, Castaneda et al. (2018) probabilistically generated the following time to corrosion initiation Equation 46, similar to the commonly used Equation 5.

$$T_{corr} = \left[\frac{c^2}{4(\alpha_1\theta_1(\theta_2)^{\theta_3})}\left[erf^{-1}\left(1 - \frac{Cth}{C_s}\right)\right]^{-2}\right]^{1/(1-\theta_3)}$$

As previously stated, there is no known single, precise value for the chloride threshold value. Therefore, the experimental work of Castro-Borges et al. (2013) involving polarization resistance techniques provided interpolated chloride threshold values at five respective water to cement ratios for Castaneda et al. (2018), which will be the assumed critical chloride values herein. These values are provided in Table 4

Table 4. Interpolated chloride threshold values

Water to Cement Ratio, WC	Interpolated Chloride Threshold Value, C_{th} (% per weight of concrete)
0.46	0.112
0.50	0.1447
0.53	0.1265
0.70	0.06797
0.76	0.0586

3.3 General corrosion

Numerical definition of corrosion propagation is provided primarily in the form of corrosion rate, which is the amount of steel loss per unit time and unit area. Most current non-destructive techniques detect corrosion utilizing an electromechanical measurement of current rate, *i*corr. Analytical models, developed by Vu and Stewart (2000), for estimating corrosion rate depend on parameters such as quality of concrete and rebar cover as given in Equation 47.

$$icorr(T) = 0.85icorr(1)T–0.29 \quad (47)$$

The time, T, indicates the time span since initiation, i.e. the initiation time of corrosion deducted from structure life. Equation 47 is viable to be used in cities located within Asian, European, American, and Australian regions due to the average relative humidity of many locations in these areas being over 70%; therefore, it is assumed that the corrosion rate is limited by the availability of oxygen at the steel surface (Vu et al. 2005). One key disadvantage of this equation is related to corrosion within makeups having short periods of structural life. If the time, T, is too small, the corrosion rate will theoretically tend to reach infinity; therefore, modified Equation 48 was put into place (Vu and Stewart 2000).

$$icorr\ (T) = \{\ icorr(1)\ 0 \le T \le 1\ year$$
$$0.85 * icorr(1) * T–0.29 \quad T > 1 year \quad (48)$$

where *i*corr(1) = One-year corrosion rate at the start of corrosion propagation (µÆ)

Developed and suggested by Dai and Wang (2009), the one-year corrosion rate is defined at the start of corrosion initiation and dependent upon variables such as the water to cement ratio and the cover of reinforcement (Equation 49).

$$icorr\ (1) = 37.8(1–WC)—1.64\ C \quad (49)$$

According to classifications recommended by BRITE/EURAM (1995), corrosion rates between 0.1 and 0.5 microamperes per square centimeter (µA/ cm2) correspond to low corrosion rates, a range of 0.5 to 1.0 µA/ cm2 correspond to moderate corrosion, and above 1.0 µA/ cm2 correspond to a high rate of corrosion. It is important to note that most reliability analyses have assumed a constant corrosion rate during the propagation period. However, Vu and Stewart (2000) rationalize that it is expected that the formation of products on the steel surface will reduce the diffusion of the iron ions away from the steel surface. Furthermore, the area ratio between the anode and the cathode is reduced. These assessments suggest that the corrosion rate will diminish with time; explicitly, more rapidly during the first few years after corrosion initiation but then at a decelerating rate as it approaches a more uniform level (Yalcyn and Ergun 1996). Data from Liu and Weyers (1998) was used in order to develop the relationship between time since corrosion initiation and the corrosion rate as seen in the aforementioned Equation 48.

ISSN 2581-9429 IJARSCT

IJARSCT
ISSN (Online) 2581-9429
International Journal of Advanced Research in Science, Communication and Technology (IJARSCT)
International Open-Access, Double-Blind, Peer-Reviewed, Refereed, Multidisciplinary Online Journal
Impact Factor: 7.301
Volume 8, Issue 1, August 2023

Bushman (2000) acknowledges that Faraday's law of electrochemical equivalence is employed into the loss of steel reinforcement when analyzing general corrosion. The reduction of diameter through the general corrosion process is indicated with Equation 50.

$$\Delta D(T) = 0.0232 * icorr(T) \quad (50)$$

where $\Delta D(T)$ = Reduction of steel reinforcement diameter (mm)

As previously mentioned, many reliability analyses rely on a constant corrosion rate within investigations. If using a constant corrosion rate, the reduction of reinforcement diameter would simply be a function of consistent corrosion multiplied by the time. Nevertheless, only a corrosion rate with respect to time will be used herein. If the corrosion current density is assumed to be identical for "n" reinforcement bars, the residual cross sectional area of rebars could be computed using Equation 51.

$$A(T) = n\pi * [D0 - \Delta D(T)]2 \geq 0 \quad (51)\ s\ 4$$

However, if the corrosion is localized as a product of pitting corrosion, the residual cross section of the rebars is found using Equation 52.

$$A\ (T) = n(\pi D\ \ 2\ \text{—}\ A\ 4) \geq 0 \quad (52)$$

3.4 Pitting corrosion

Tutti (1982) and Gonzalez et al. (1995) have been significant developers of modeling pitting corrosion within chloride-contaminated structures. Stewart (2004) mentions that the maximum pit depth, *P*max, will normally exceed the penetration calculated based on general corrosion, *P*av. Researchers indicate, however, that there is a significant uncertainty associated with this with this ratio. Gonzalez et al. (1995) found in a study where concrete specimens were exposed to natural environments that the maximum ratio of maximum pit depth to penetration of general corrosion, denoted as R, tended to vary from 4 to 8. The results of Gonzalez et al. (1995) were in broad agreement with Tutti (1982) who suggested that the ratio usually falls within a range of 4 to 10.

Darmawan and Stewart (2003) have found the distribution of maximum pit depths for prestressing wires has found to be best represented by the Gumbel (Extreme Value-Type I) distribution. Extreme value statistics have been widely used to characterize the pitting of steel plates and pipes as well as prestressing strands. Therefore, it is reasonable that the Gumbel distribution be appropriate for modeling maximum pit depths of reinforcing bars (Stewart 2004).

A popular approach in modeling pit depth using extreme value theory originates from Turnbull (1993). The ratio of maximum pit depth to average penetration from general corrosion, R, is treated as a random variable modeled by the Gumbel distribution using Equation 53. This random variable is also referred to as the pitting factor

$$F(R) = e\text{–e—}(R\text{—}\mu)/\alpha \quad (53)$$

where μ = Location parameter

α = Scale parameter

The location and scale parameters characterize the spread of the distribution. According to Stewart (2004), these parameters can be determined, grounded on the results of Gonzalez et al. (1995), that for an 8 millimeter diameter bar of 125 millimeter length, R=4 and R=8 represent the 5th and 95th percentiles of the distribution, respectively. The mean and coefficient of variation are then considered to correspondingly be 5.65 and 0.22, which relate to the parameters of the Gumbel distribution $\mu 0$=5.08 and $\alpha 0$=1.02. Turnbull (1993) suggests that for a reinforcing bar with different dimensions, the Gumbel distribution parameters can be determined using Equations 54 and 55. The mean and standard deviation are related to these parameters by Equations 23 and 24.

$$\mu = \mu 0 + 1\ ln\ (\text{Æ}) \quad (54)$$

$$\alpha 0\ \text{Æ}0\ \alpha = \alpha 0 \quad (55)$$

where A = surface area of the respective bar

$A0$ = surface area of an 8mm diameter bar of 125 mm length

With the distribution factors of random variable of R, the maximum pit depth along a reinforcing bar can be evaluated using Equation 56.

$$P(T) = 0.0116 * icorr(T) * R * T \quad (56)$$

IJARSCT
ISSN (Online) 2581-9429
International Journal of Advanced Research in Science, Communication and Technology (IJARSCT)
International Open-Access, Double-Blind, Peer-Reviewed, Refereed, Multidisciplinary Online Journal
Impact Factor: 7.301
Volume 8, Issue 1, August 2023

This equation considers Faraday's law where a unit current density induces a uniform corrosion penetration of 11.6 micrometers per year (El Hassan et al. 2010). A model to predict the loss of the cross-sectional area of a reinforcing bar due to pitting has been proposed by Val and Melchers (1997). The pit configurations, as seen in Figures 10 and 11, the width of the pit, and cross sectional area of the pit can be expressed using Equations 57-62.

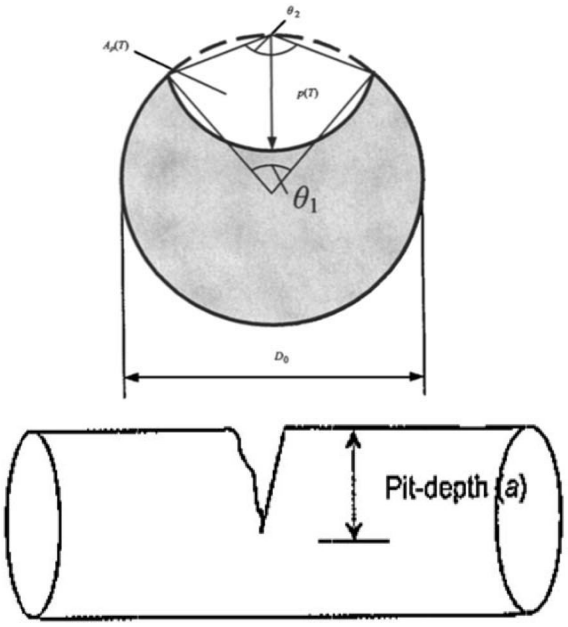

IV. TIME TO CORROSION INITIATION

The time to corrosion initiation was estimated using Equation 46 and Tables 1-6. However, in Equation 46, there are multiple random variables with a normal distribution type, which allow for irregularity within a design space. Though realistic and representative to the premise that no design space with the same materials or mechanical properties will have the same precise time to corrosion initiation, the average value from 10,000 simulations of Equation 46 was utilized for each design space with three varying concrete covers and three separate water to cement ratios. For the purpose of consistency, these average values were modeled as the beginning of the life of a structure before corrosion propagation within instances of general and pitting corrosion, which can be seen in the following sections. Using MATLAB scripts, the approximate values of time to corrosion initiation for each considered occurrence can be seen in Figures 12-20 below. Whether the design space undergoes pitting or general corrosion is redundant; therefore, the only parameters necessary to analyze the time to corrosion initiation is the water to cement ratio and concrete cover. These figures clearly portray that the time to corrosion initiation decreases with a lower concrete cover and a higher water to cement ratio.

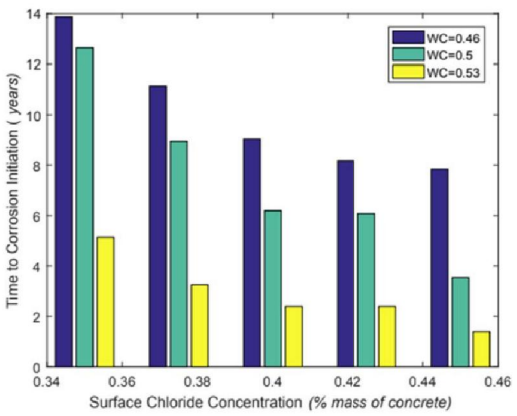

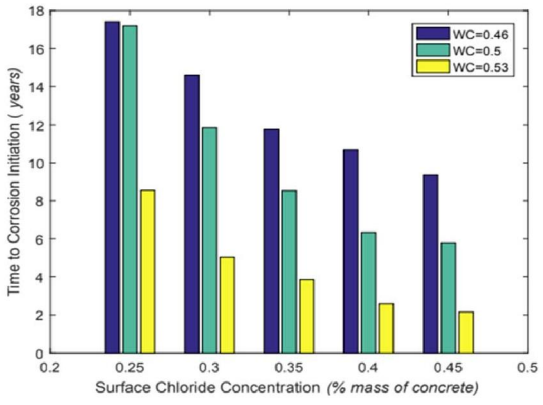

IJARSCT
ISSN (Online) 2581-9429
International Journal of Advanced Research in Science, Communication and Technology (IJARSCT)
International Open-Access, Double-Blind, Peer-Reviewed, Refereed, Multidisciplinary Online Journal
Impact Factor: 7.301
Volume 8, Issue 1, August 2023

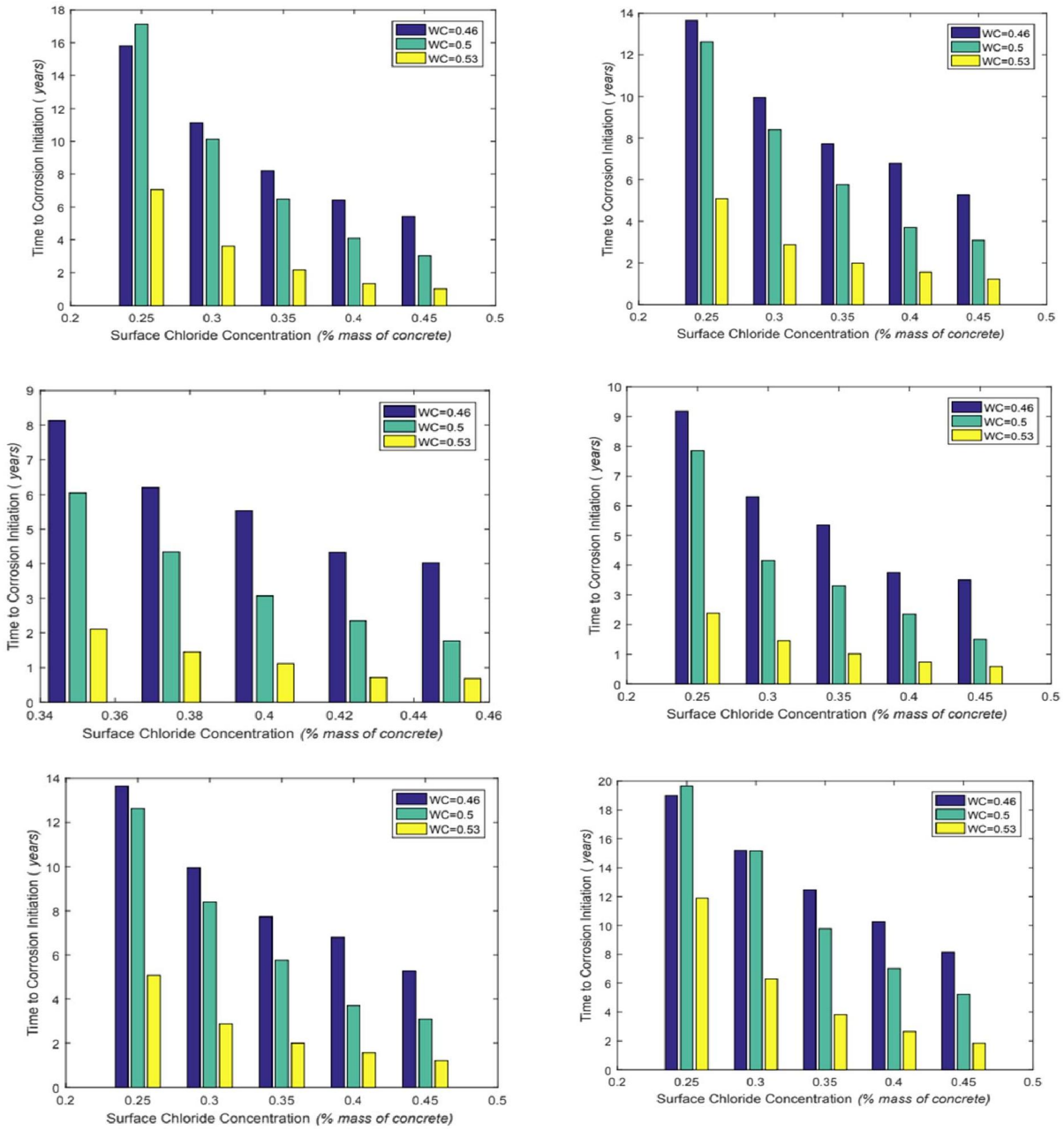

4.1 Moment values for each Dead to Live Ratio

The dead and live load moments, considered as the load effects of the limit state function, are estimated for each considered design using Equations 63, 68, and 70. Both the dead and live loads are represented as random variables within the limit state function. Different dead to live load ratios were evaluated for each design space, and respective dead and live load values that satisfy the design equation were computed at each ratio. Thus, producing new values to each variable already containing randomness, it is expected that the FORM procedure will produce distinctions in the reliability index for each ratio because of their difference statistical characteristics. The values for each dead and live load moment, as well as a consistent ultimate moment value, can be reviewed for each design space from Tables 7-9.

IJARSCT
ISSN (Online) 2581-9429
International Journal of Advanced Research in Science, Communication and Technology (IJARSCT)
International Open-Access, Double-Blind, Peer-Reviewed, Refereed, Multidisciplinary Online Journal
Impact Factor: 7.301
Volume 8, Issue 1, August 2023

M_D/M_L	M_D (kN*m)	M_L (kN*m)	M_n (kN*m)	$\varphi * M_n = M_u$(kN*m)
0.5	1245	2490		
0.75	1651	2201		
1	1971	1971		
1.25	2232	1785		
1.5	2447	1632		
1.75	2629	1502	6572	5914
2	2783	1392		
2.25	2917	1296		
2.5	3033	1213		
2.75	3135	1140		
3	3226	1075		

M_D/M_L	M_D (N*m)	M_L (N*m)	M_n (N*m)	$\varphi * M_n = M_u$
0.5	736.0	1472		
0.75	975.7	1301		
1	1165	1165		
1.25	1319	1055		
1.5	1447	964.5		
1.75	1554	887.9	3885	3496
2	1645	822.6		
2.25	1724	766.3		
2.5	1793	717.2		
2.75	1853	674.0		
3	1907	635.7		

M_D/M_L	M_D (N*m)	M_L (N*m)	M_n (N*m)	$\varphi * M_n = M_u$
0.5	431.7	863.4		
0.75	572.3	763.0		
1	683.5	683.5		
1.25	773.8	619.0		
1.5	848.5	565.7		
1.75	911.4	520.8		
2	965.0	482.5		
2.25	1011	449.4	2278	2051
2.5	1052	420.6		
2.75	1087	395.3		
3	1118	372.8		

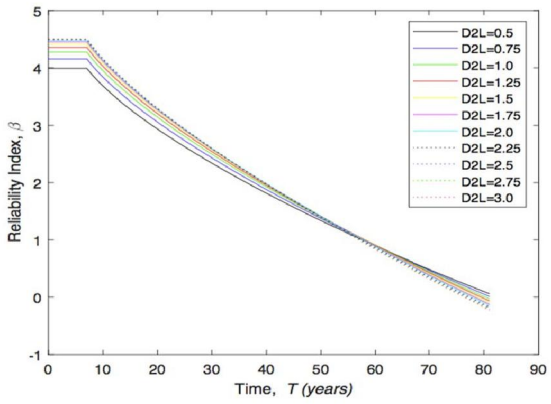

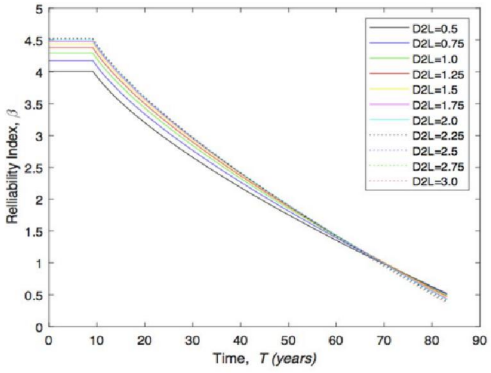

V. EXPERIMENTAL SETUP

5.1 Design of Beam Specimen

Eight reinforced concrete cantilever beams with OPC of dimension 300mm x 400mm in cross section and 2150mm in length have been casted. The behaviour of reinforced concrete beams of 2.5%, 5%, and 7.5% corrosion will be studied. Two beams are casted as control specimen (i.e., 0% corrosion). The details of experimental program, materials used, and method of testing is explained below.

IJARSCT
ISSN (Online) 2581-9429
International Journal of Advanced Research in Science, Communication and Technology (IJARSCT)
International Open-Access, Double-Blind, Peer-Reviewed, Refereed, Multidisciplinary Online Journal
Impact Factor: 7.301
Volume 8, Issue 1, August 2023

PROPORTION OF MATERIALS

Sr. No	Content	Weight (kg/m3)	Proportion
1)	Water	164.80 lit	0.51
2)	Cement	320.00	1
3)	Fine aggregate	704.72	2.20
4)	Coarse Aggregate	1176.35	3.67

DESIGN STIPULATION FOR MIX DESIGN

Sr. No	Description	Design Standard
1)	Grade designation	20 MPa
2)	Type of cement	OPC-43
3)	Fine aggregate	Zone-II
4)	Specific gravity of cement	3.14
5)	Specific gravity of fine aggregate	2.56
6)	Specific gravity of coarse aggregate	2.66

5.2 Testing Procedure

The RC beam specimens were casted as specified. In the present study 2 control specimens and 6 uncontrolled specimens (2.5%,5%,7.5% of corrosion) prepared with OPC mix were tested as a cantilever beam, in the specially prepared loading setup, to determine the flexural capacity. Hydraulic jack was used to fix the beam bottom to the reaction bed. Here we measured deflection, strain and crack using dial guage, strain guage and crack measuring microscope respectively.

Results

a) Corrosion Rate Measurements

The beam specimens were divided into number of grids to locate the guard ring probe to polarize the definite area on concrete rebar as shown in the fig 2. At each node, corrosion current density was measured by LPR technique. The current density for each control specimen is shown in the Table 3.

IJARSCT
ISSN (Online) 2581-9429
International Journal of Advanced Research in Science, Communication and Technology (IJARSCT)
International Open-Access, Double-Blind, Peer-Reviewed, Refereed, Multidisciplinary Online Journal
Impact Factor: 7.301
Volume 8, Issue 1, August 2023

CORROSION CURRENT DENSITY OF SPECIMENS.

		Corrosion current density, (mA/cm²)					
	Grid Number	1	2	3	4	5	Avg
Beams	Control Beam	0.003 7	0.0038	0.0042	0.0039	0.0042	0.0039
	2.5% Corroded Beam	0.03	0.0330	0.02599	0.0248	0.06059	0.0351
	5% Corroded Beam	0.0438	0.05326	0.0356	0.0432	0.0468	0.0409
	7.5% Corroded Beam	0.0623	0.0682 6	0.0658	0.07082	0.072	0.067

Table 4 Corrosion current density of Specimens.

b) Ultimate Load and Deflection

ULTIMATE LOAD & DEFLECTION OF BEAMS

Beam Specimen	Ultimate Load (KN)	Average Ultimate Load (KN)	Deflection (mm)	Average Deflection (mm)
0%	93.9	92.87	60.67	60.60
	91.8		61.55	
	92.9		59.58	
2.5%	89.96	87.12	80.35	76.72
	86.17		73.91	
	85.23		75.91	
5%	85.23	84.91	82.36	74.36
	84.28		61.18	
	85.23		79.56	
7.5%	72.38	72.38	85.65	77.27
	76.19		71.51	
	68.57		74.65	

5.3 Development of Corrosion Assessment Model

After 45 days of exposure, accumulation of rust was observed on the surface of all the specimens. Figs. 6 (a and b) show the condition of specimen 5 (reference specimen) in the pristine state and after accelerated chloride exposure of 45days. To examine the condition of the concrete and the rebar inside it, the specimen was cut open at 45 days as shown in Fig. 6 (c). The corrosion initiation is clearly visible as the red rust, in both the steel rebar as well as in the concrete at the steel/concrete interface. As apparent from the figures, it can be concluded that the corrosion had already initiated by the 45th day. After this observation, the other specimens (numbered 1-4) were continued in the accelerated corrosion environment until cracks were developed on the surface of the cubes. Substantial cracks appeared in all the RC cubes after 120 days of exposure, as shown for typical specimen1 in Fig. 6 (a). This happened due to the accumulation of the corrosion products, creating an expansive stress exceeding the tensile strength of concrete. To examine the condition of the rebar and the concrete inside the specimen, all the remaining specimens (1 to 4) were split open and the rebars were removed to carry out the gravimetric mass loss measurements. Figs. 6 (b and c) show the condition of the rebar and the surrounding concrete for a typical specimen 1 split open after 120 days. Figure 6 Condition of RC specimen 5 (a) Pristine state (b) After 45 days (c) After split open at 45 days Figure 6 Condition of specimen 1 after 120 days of accelerated corrosion.

IJARSCT
ISSN (Online) 2581-9429
International Journal of Advanced Research in Science, Communication and Technology (IJARSCT)
International Open-Access, Double-Blind, Peer-Reviewed, Refereed, Multidisciplinary Online Journal
Impact Factor: 7.301
Volume 8, Issue 1, August 2023

(a) (b) (c)

Condition of RC specimen 5 (a) Pristine state (b) After 45 days (c) After split open at 45 days

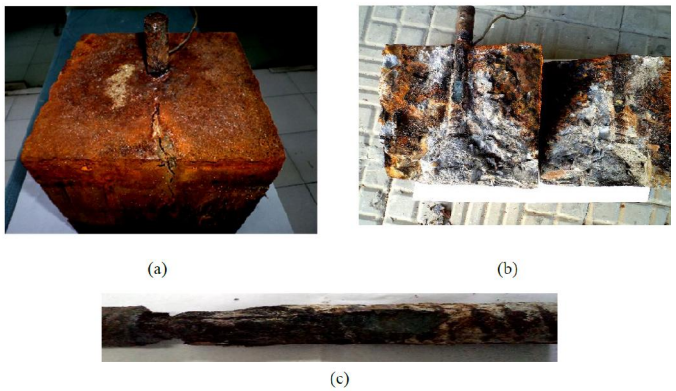

(a) (b) (c)

Condition of specimen 1 after 120 days of accelerated corrosion (a) Cracked specimen (b) Cracked specimen after splitting (c) Corroded bar

VI. SUMMARY AND CONCLUSION

6.1 Summary

Structural reliability methods can provide a probabilistic risk assessment of the structural integrity of infrastructure and offer insight on the vulnerability of structures corresponding to particular levels of demand they must resist. There are numerous statistical methods and simulation techniques that employ the reliability theories to approximate the structural reliability of a structure during its service life. In this study, typical reinforced concrete girders were analyzed using the First Order Reliability Method from three different bridge configurations undergoing particular corrosion conditions to assess how the mechanical and material properties would affect the reliability of each respective element over its' intended service life.

6.2 Conclusion

The results above clearly show the impact of the concrete cover and water to cement ratio and how these parameters can affect other mechanical properties and performance of a structure over time within corrosion processes. Increasing the concrete cover is the most inexpensive and practically feasible way to protect the reinforcing steel from corrosion and sustain its' structural integrity over a prolonged period. It is crucial to identify the nature of corrosion that reaches steel reinforcement as soon as possible in order to best evaluate methods for repair, especially in instances of pitting corrosion due to the rapid decline of residual area that can happen in areas of importance.

From the experimental investigation it is observed that the load carrying capacity of the beam is more for control beams, but Deflection is less for Control beams with respect to Corroded beams (2.5%, 5%, and 7.5%). It is concluded that, as the rate of corrosion increases above 5%, the Ductility property of beam specimen goes on reducing. It is observed that the Moment Carrying Capacity of control beams is more, with respect to Corroded beams (2.5%, 5%, and 7.5%)

The peak load and the Strains sustained by the Control beams is more than the Corroded beams. The Moment Carrying Capacity was less for corroded Beams with respect to Control Beams. But the Curvature observed was more for Corroded Beams. The number of cracks developed is more in case of Control Beams as that of Corroded Beams, but as the rate of corrosion increases the crack width increases in Corroded Beams than in Control Beams.

IJARSCT
ISSN (Online) 2581-9429
International Journal of Advanced Research in Science, Communication and Technology (IJARSCT)
International Open-Access, Double-Blind, Peer-Reviewed, Refereed, Multidisciplinary Online Journal
Impact Factor: 7.301
Volume 8, Issue 1, August 2023

VII. RECOMMENDATIONS FOR FUTURE RESEARCH

The proposed methodology could be used as a decision-making tool that allow infrastructure owners and managers to prioritize repair needs and budget allocations based on time at which a certain reliability threshold will be reached. Additional research should be done on this topic to evaluate the reliability of a structure with increased accuracy. First and foremost, this research only analyzed the loss steel reinforcement and its effects on the flexural strength of structures undergoing corrosion mechanisms. This framework can be taken a step further by identifying manners on how corrosion impairs the surrounding concrete strength as well. With regards to this exclusive study, the definition of the chloride threshold should be specified more clearly in order to be able to accurately quantify this variable. Also, the model used in this research suggested that the pitting factor was deterministic for each bar of steel reinforcement across the entirety of the span length. This is an area within pitting corrosion that can see development, as it is not likely that each individual bar will have similar pitting depths. Another future calibration could also include contrasting current densities within the cross section of a featured area, where reinforcement closer to edges will likely receive a higher corrosion density and thus, a higher probability of failure for those particular elements. Lastly, effects of environmental conditions such as temperature, humidity, and location could be studied to reflect how the climate of a structures' location will influences serviceability.

The following tasks are recommended to be undertaken to continue the research further

1. The present work was carried out on normal strength concrete; the same can be extended to high strength concrete and using different grades of steel.
2. The developed corrosion model can be validated, based on the measurements of corrosion from real life structures for long term effects, spanning at least for ten years, so as to cover the corrosion propagation and cracking phase.
3. The equivalent parameters developed can be compared with analytical results for simple structures.
4. Research may focus on Remaining Service life prediction of the RC structure based on the developed models for chloride and carbonation induced corrosion.

REFERENCES

[1]. AASHTO LRFD Bridge Design Specifications. Washington, D.C. :American Association of State Highway and Transportation Officials, 2017. Print.

[2]. Allen T.M., Nowak A.S., Bathurst R.J. 2005. Calibration to Determine Load and Resistance Factors for Geotechnical and Structural Design. Transportation Research E-Circular(E-C079).

[3]. Almusallam A A. Effect of degree of corrosion on the properties of reinforcing steel bars.

[4]. Construction and Building Materials 2001; 15(8): 361-368, https://doi.org/10.1016/S0950-0618(01)00009-5.

[5]. Bastidas-Arteaga E, Bressolette P, Chateauneuf A, Sánchez-Silva M. Probabilistic lifetime assessment of RC structures under coupled corrosion–fatigue deterioration processes. Structural Safety 2009; 31(1): 84-96, https://doi.org/10.1016/j.strusafe.2008.04.001.

[6]. Bastidas-Arteaga E, Sánchez-Silva M, Chateauneuf A, Silva M R. Coupled reliability model of biodeterioration, chloride ingress and cracking for reinforced concrete structures. Structural Safety 2008; 30(2): 110-129, https://doi.org/10.1016/j.strusafe.2006.09.001.

[7]. Bertolini, L., Elsener, B., Pedeferri, P., Redaelli, E., and Polder, R. (2018). Corrosion of Steel in Concrete - Prevention, Diagnosis, Repair (2nd Edition), John Wiley & Sons.

[8]. Bhargava, K., Mori, Y., and Ghosh, A. K. (2011). "Time-dependent reliability of corrosion-affected RC beams—Part 1: Estimation of time-dependent strengths and associated variability." Nuclear Engineering and Design, 241, 1371-1384. CRC Press, Cambridge, England Boca Raton.

[9]. BRITE/EURAM. (1995). "The residual service life of reinforced concrete structures." Final Technical Rep. BRUE CT92-0591, Brite/EURAM, European Union.

[10]. Bushman J B, Engineer P P. Calculation of Corrosion Rate from Corrosion Current (Faraday's Law). Bushman & Associates Inc. 2000.

IJARSCT
ISSN (Online) 2581-9429
International Journal of Advanced Research in Science, Communication and Technology (IJARSCT)
International Open-Access, Double-Blind, Peer-Reviewed, Refereed, Multidisciplinary Online Journal
Impact Factor: 7.301
Volume 8, Issue 1, August 2023

[11]. Cairns, J., Plizzari, G. A., Du, Y. G., Law, D. W., and Franzoni, C. (2005). "Mechanical properties of corrosion-damaged reinforcement." 256-264.

[12]. Castaneda, Homero; Karsilaya, Aydin; Okeil, Ayman; and Taha, Mahmoud Reda, (2018). Publications. 26. https://digitalcommons.lsu.edu/transet_pubs/26.

[13]. Castro-Borges, P., Balancán-Zapata, M., López-González, A. Analysis of Tools to Evaluate Chloride Threshold for Corrosion Onset of Reinforced Concrete in Tropical Marine Environment of Yucatán, México, J. Chem. 2013 (2013) 1–8. doi:10.1155/2013/208619.

[14]. Cicek, V.: Corrosion Engineering and Cathodic Protection Handbook. Wliey, Hoboken (2017).

[15]. Dai H, Wang W. Application of low-discrepancy sampling method in structural reliability analysis. Structural Safety 2009; 31(1): 55-64, https://doi.org/10.1016/j.strusafe.2008.03.001.

[16]. Darmawan MS, Stewart MG. Spatial variability of pitting corrosion and its effect on the reliability of prestressing wires. In: Der Kiureghain A, Madanat S, Pestana JM, editors. Nineth International Conference on Applications of Statistics and Probability in Civil Engineering, 1. Rotterdam: Millpress; 2003. p. 541–8.

[17]. Darmawan, M. S. (2010). "Pitting corrosion model for reinforced concrete structures in a chloride environment." 91-101.

[18]. Dolinski, K. 1982. First Order Second Moment Approximation in Reliability of Structural Systems: Critical Review and Alternative Approach.

[19]. Drewett, J.; Broomfield, J.: An introduction to electrochemical rehabilitation techniques.

[20]. Technical Note 2. CPA Technical Note (2011).

[21]. DuraCrete. Probabilistic performance based durability design of concrete structures. The European Union-Brite EuRam III Project BE95-1347; 2000.

[22]. Ellingwood B. Development of a probability based load criterion for American National Standard A58: Building code requirements for minimum design loads in buildings and other structures. US Department of Commerce, National Bureau of Standards; 1980, https://doi. org/10.6028/nbs.sp.577.

[23]. Elsener, B., and Angst, U. (2007). "Mechanism of electrochemical chloride removal." Corrosion Science, 49, 4504-4522.

[24]. Frangopol, Dan M., and Allen C. Estes. "Lifetime Bridge Maintenance Strategies Based on System Reliability." Structural Engineering International, vol. 7, no. 3, Aug. 1997, p. 193.

[25]. Geiker, M. R., and Polder, R. B. (2016). "Experimental support for new electro active repair method for reinforced concrete." Materials & Corrosion / Werkstoffe und Korrosion, 67(6), 600-606.

[26]. Ghanooni-Bagha, M., Shayanfar, M. A., Reza-Zadeh, O., and Zabihi-Samani, M. (2017). "The Effect Of Materials On The Reliability Of Reinforced Concrete Beams In Normal And Intense Corrosions." Wpływ Stosowanych Materiałów Na

[27]. Niezawodność Belek Żelbetowych W Warunkach Normalnej I Silnej Korozji., 19(3), 393.

[28]. Gonzalez JA, Andrade C, Alonso C, Feliu S. Comparison of rates of general corrosion and maximum pitting penetration on concrete embedded steel reinforcement. Cement Concrete Research1995;25(2):257–64.

[29]. Goyal, A., Pouya, H. S., Ganjian, E., Claisse, P. J. A. J. f. S., and Engineering (2018). "A Review of Corrosion and Protection of Steel in Concrete." 43(10), 5035-5055.

[30]. Hasaan, J., Bressolette P., Cheateauneuf, A., El Tawil, K. Reliability-based assessment of the effect of climatic conditions on the corrosion of RC structures subject to chloride ingress. 2010.

[31]. Heiyantuduwa, R., Alexander, M. G., and Mackechnie, J. R. (2006). "Performance of a Penetrating Corrosion Inhibitor in Concrete Affected by Carbonation-Induced Corrosion." Journal of Materials in Civil Engineering, 18(6), 842-850.

[32]. Holicky, 2009. Reliability Analysis for Structural Design.

[33]. Kaszyńska M.,Nowak A.S.,TargetReliabilityforDesignandEvaluationof Bridges, Proceedings of the Conference on Bridge Management 5, ed. Parke, G.A.R. and Disney, P. at University of Surrey, U.K., April 2005, pp. 401-408.

[34]. Kaukaas. 2018. Mean Value First Order Second Moment Method (MVFOSM).

IJARSCT
ISSN (Online) 2581-9429
International Journal of Advanced Research in Science, Communication and Technology (IJARSCT)
International Open-Access, Double-Blind, Peer-Reviewed, Refereed, Multidisciplinary Online Journal
Impact Factor: 7.301
Volume 8, Issue 1, August 2023

[35]. Koch, G. H. et al. Corrosion Cost and Preventative Strategies in the United States. Report No. FHWA-RD-01-156, 773 (NACE International, Houston, 2002).
[36]. Liberati, E. A. P., Leonel, E. D., and Nogueira, C. G. (2014). "Influence of the
[37]. reinforcement corrosion on the bending moment capacity of reinforced concrete beams: a structural reliability approach." Revista IBRACON de Estruturas e Materiais, Vol 7, Iss 3, Pp 379-413(3), 379.
[38]. Liu T, Weyers RE. Modeling the dynamic corrosion process in chloride contaminated concrete structures. Cement and Concrete Research 1998;28(3):365-79.
[39]. Markeset and Mydral. Modeling of Reinforcement Corrosion in Concrete – State of the Art. 2008.
[40]. Marques, P.F.; Costa, A.: Service life of RC structures: carbonation induced corrosion.
[41]. Prescriptive vs. performance-based methodologies. Constr. Build. Mater. 24, 258– 265 (2010). https://doi.org/10. 1016/j.conbuildmat.2009.08.039
[42]. Nogueria et al. Probabilistic Failure Modeling of Reinforced Concrete Structures Subjected to Chloride. 2012.
[43]. Nóvoa, X. (2016). "Electrochemical aspects of the steel-concrete system. A review." Journal of Solid State Electrochemistry, 20(8), 2113-2125.
[44]. Nowak, A. S. (1999). "Calibration of LRFD bridge design code." NCHRP Rep. No. 368, Transportation Research Board, Washington, DC, 37.
[45]. Nowak, A. S., and Collins, K. R. (2000). Reliability of structures, McGraw- Hill, New York.
[46]. Nowak, A. S., and Szerszen, M. M. (2003). "Calibration of design code for buildings (ACI 318): Part 1. Statistical models for resistance." ACI Struct. J., 100(3), 377–382.
[47]. Okeil, Ayman M., et al. "Reliability Assessment of FRP-Strengthened Concrete Bridge
[48]. Girders in Shear." Journal of Composites for Construction, vol. 17, no. 1, Jan. 2013, pp. 91-100. EBSCOhost, doi:10.1061/(ASCE)CC.1943-5614.0000315.
[49]. Östlund L. An estimation of γ-values. Bulletin du Comité Euro-international du Béton 1991(202): 38-97.
[50]. Popov, B. N. (2015). "Chapter 1 - Evaluation of Corrosion." Corrosion Engineering, B. N. Popov, ed., Elsevier, Amsterdam, 1-28.
[51]. Poupard, O., Aït-Mokhtar, A., and Dumargue, P. (2004). "Corrosion by chlorides in reinforced concrete: Determination of chloride concentration threshold by impedance spectroscopy." Cement & Concrete Research, 34(6), 991.
[52]. Shayanfar, M. A., Barkhordari, M. A., and Ghanooni-Bagha, M. (2015). "Estimation of Corrosion Occurrence in RC Structure Using Reliability Based PSO Optimization." 531-542.
[53]. Stewart MG. Spatial variability of pitting corrosion and its influence on structural fragility and reliability of RC beams in flexure. Structural Safety 2004;26(4):453– 70.
[54]. The Concrete Society: Guidance on the use of stainless steel reinforcement. Concrete Society, TR 51 (1998)
[55]. Turnbull, A. (1993). "Review of modeling of pit propagation kinetics." Br. Corros. J., London, 28(4), 297–308.
[56]. Tutti, K. (1982). "Corrosion of Steel in Concrete " CBI Swedish Cement and Concrete Institute 469.
[57]. Val DV. Deterioration of strength of RC beams due to corrosion and its influence on beam reliability. J Struct Eng, ASCE 2007;133(9):1297–306
[58]. Val DV, Melchers RE. Reliability of deteriorating RC slab bridges. J Struct Eng ASCE 1997;123(12):1638–44.
[59]. Vu K, Stewart M G, Mullard J. Corrosion-induced cracking: experimental data and predictive models. ACI Structural Journal 2005; 102(5): 719-726.
[60]. Vu K A, Stewart M G. Structural reliability of concrete bridges including improved chloride-induced corrosion models. Structural Safety 2000; 22(4): 313-333, https://doi.org/10.1016/S0167-4730(00)00018-7.
[61]. Wong. 1984. First-Order, Second Moment Methods.